Current Biology, Vol. 12, 1405–1412, August 20, 2002, ©2002 Elsevier Science Ltd. All rights reserved. PII S0960-9822(02)01044-8

Analysis of a Zebrafish VEGF Receptor Mutant Reveals Specific Disruption of Angiogenesis

Hinrich Habeck,[1] Jörg Odenthal,[1] Brigitte Walderich,[1] Hans-Martin Maischein,[2] *Tübingen 2000 screen consortium*,[4] and Stefan Schulte-Merker[1,3]

[1]Artemis Pharmaceuticals/Exelixis Deutschland GmbH

[2]Max-Planck-Institut für Entwicklungsbiologie
Abteilung Genetik
Spemannstr. 35
72076 Tübingen
Germany

Summary

Blood vessels form either by the assembly and differentiation of mesodermal precursor cells (vasculogenesis) or by sprouting from preexisting vessels (angiogenesis) [1–3]. Endothelial-specific receptor tyrosine kinases and their ligands are known to be essential for these processes. Targeted disruption of vascular endothelial growth factor (VEGF) or its receptor kdr (flk1, VEGFR2) in mouse embryos results in a severe reduction of all blood vessels [4–6], while the complete loss of flt1 (VEGFR1) leads to an increased number of hemangioblasts and a disorganized vasculature [7, 8]. In a large-scale forward genetic screen, we identified two allelic zebrafish mutants in which the sprouting of blood vessels is specifically disrupted without affecting the assembly and differentiation of angioblasts. Molecular cloning revealed nonsense mutations in *flk1*. Analysis of mRNA expression in *flk1* mutant embryos showed that *flk1* expression was severely downregulated, while the expression of other genes (*scl*, *gata1*, and *fli1*) involved in vasculogenesis or hematopoiesis was unchanged. Overexpression of $vegf_{121+165}$ led to the formation of additional vessels only in sibling larvae, not in *flk1* mutants. We demonstrate that *flk1* is not required for proper vasculogenesis and hematopoiesis in zebrafish embryos. However, the disruption of *flk1* impairs the formation or function of vessels generated by sprouting angiogenesis.

Results

Identification of Mutations with Specific Vascular Defects

In a large-scale genetic screen, we used the endogenous alkaline phosphatase activity of zebrafish endothelial cells to visualize blood vessels at 4 days postfertilization (dpf) [9, 10]. We examined the F3 progeny of males mutagenized with ethylnitrosourea (ENU) for changes in blood vessel formation and identified more than 700 mutants (4.521 mutagenized genomes screened).

Two allelic mutants, *t20257* and *t21588*, displayed identical vascular defects. Because the results of the phenotypic analysis were identical for both alleles, we show here data for *t20257*. In mutant embryos, the overall morphology appeared to be normal up to 4 dpf (Figures 1A and 1B). After this time point, a heart edema of increasing size formed, and the larvae became necrotic and died approximately at 7 dpf. Alkaline phosphatase staining revealed specific defects of the vasculature (Figures 1C–1F). The intersegmental vessels (Se) were either missing or just reached the horizontal myoseptum in most cases, and the Se spanned the entire lateral aspect of the larva at only a few somatic boundaries (Figures 1C and 1D). The parachordal vessels (PAV) were well developed in mutants and connected the shortened Se. The subintestinal vein (SIV) was thin and often interrupted (Figures 1E and 1F), and the number of branches spanning the yolk was reduced. The changes of the Se and the SIV were variable.

Additionally, starting at 3 dpf, we observed in approximately 30% of the mutant larvae accumulations of erythrocytes either around the eyes or the developing swim bladder (Figures 1G–1J).

Vessels Forming Later than 36 hpf Are Reduced or Absent in *t20257* Mutant Embryos

A detailed analysis of the vascular defects of *t20257* and a test for functionality of vessels was done by using the microangiography technique [11, 12]. At 26 hpf, the circulation in zebrafish is established, and, at this stage of development, mutant and sibling larvae were indistinguishable by microangiography (data not shown). The first alterations in the mutants became visible at 2 dpf. At this stage, the Se have luminized at every somite boundary in wild-type embryos. In mutant embryos, however, only about 50% of somite boundaries had at least one out of two bilateral Se that reached the most dorsal region. At the other somite boundaries, the Se were absent or stopped prematurely. All vascular defects remained and could clearly be seen at 4 dpf (Figures 2A and 2B). In contrast to alkaline phosphatase staining, only the most proximal parts of the SIV were detectable by microangiography, and this proved that the main part of this vessel was without continuous circulation. Also, the pectoral fins lacked the vascular loop consisting of the pectoral artery and vein (Figures 2A and 2B).

The head vessels in *t20257* mutant embryos developed normally up to 1.5 dpf and established all main routes of blood supply (data not shown). After 1.5 dpf in the wild-type, the central arteries start to sprout, penetrate into the brain substance, and form a complex network [12]. In mutant embryos, none of the central arteries

[3]Correspondence: s.schulte@artemispharma.de

[4]*Tübingen 2000 screen consortium*: Max-Planck-Institut für Entwicklungsbiologie: Bebber van, F., Busch-Nentwich, E., Dahm, R., Frohnhöfer, H.-G., Geiger, H., Gilmour, D., Holley, S., Hooge, J., Jülich, D., Knaut, H., Maderspacher, F., Neumann, C., Nicolson, T., Nüsslein-Volhard, C., Roehl, H., Schönberger, U., Seiler, C., Söllner, C., Sonawane, M., Wehner, A., and Weiler, C.; Artemis Pharmaceuticals/Exelixis Deutschland GmbH: Hagner, U., Hennen, E., Kaps, C., Kirchner, A., Koblizek, T.I., Langheinrich, U., Metzger, C., Nordin, R., Pezzuti, M., Schlombs, K., deSantana-Stamm, J., Trowe, T., Vacun, G., Walker, A., and Weiler, C.

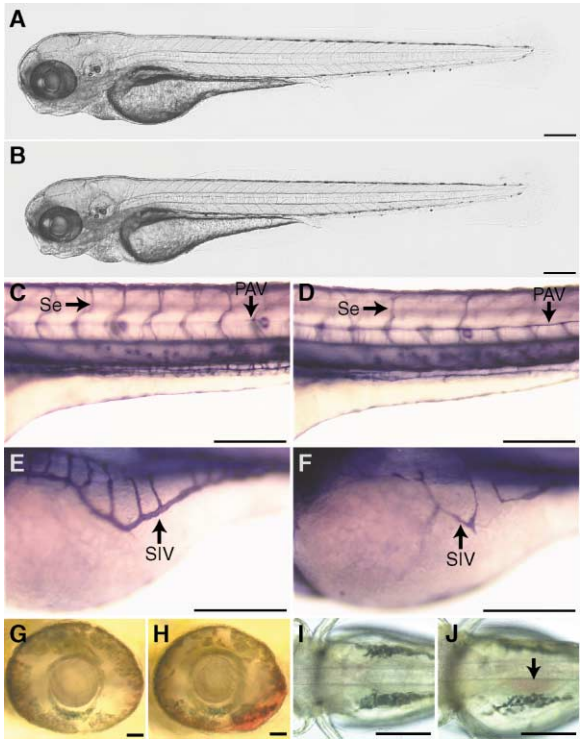

Figure 1. Various Aspects of the Vasculature Are Affected in *t20257* Mutant Larvae

(A–J) (A, C, E, G, and I) Sibling larvae and (B, D, F, H, and J) *t20257* mutant larvae at 4 dpf (PTU treated). (A and B) Mutant larvae display no obvious overall morphological changes. (C–F) Alkaline phosphatase staining reveals the reduction of intersegmental vessels (Se) and the subintestinal vein (SIV) in *t20257* mutants (PAV: parachordal vessel). (G–J) In some mutant larvae, erythrocytes accumulate either (G and H) around the eyes or (I and J) above the yolk sac. The scale bar represents 200 μm in (A)–(F), (I), and (J) and 40 μm in (G) and (H).

could be detected in microangiographies at 4 dpf, while the vessels with a large diameter formed before 1.5 dpf developed normally (Figures 2C–2F). A remarkable exception was the lateral dorsal aorta. In wild-type larvae, the section between the efferent artery of the first branchial arch and the caudal division of the internal carotid artery consists of a single vessel. In contrast, in mutant larvae, a vascular plexus of variable size formed (Figures 2G and 2H).

In summary, the analysis of the circulatory system shows that, in *t20257* mutants, the development of vessels was unaltered up to 1.5 dpf. All vessels that are either reduced, absent, or not functional in *t20257* mutants form after this time point.

Molecular Cloning Reveals a Mutation in the Gene Previously Published as *flk1*

The allele *t20257* mapped to linkage group 14 between microsatellite marker z1226 and z36206 (Figure 3A). Radiation hybrid mapping data [13] showed that a gene fragment published as *flk1* [14–17] mapped in this interval. We assembled a contiguous stretch of genomic DNA covering the whole locus (Figure 3A) and generated a simple sequence length polymorphism marker (HH01). For this marker, no recombination event could be observed in 3.122 meioses. We also performed 5′RACE for *flk1* and obtained the full-length sequence.

To determine if a knockdown of *flk1* mimics the mutant phenotype, we injected antisense morpholino oligonucleotides targeting the 5′ UTR of *flk1*. Larvae injected with 4.5 ng morpholino displayed the same vascular defects as observed in *t20257* mutant larvae without changing the overall morphology (Figures 3B, 3D, and 3F), while injection of control morpholinos had no effect (Figures 3C and 3E). This finding strongly suggested that *t20257* and *t21588* carry mutations in the *flk1* gene.

By sequencing *flk1* cDNA from *t20257* mutant larvae, we found a T-to-A transversion changing a leucine codon (amino acid 601) into a stop codon, while, in *t21588*, a C-to-A transversion changes a cysteine codon (amino acid 470) into a stop codon. These single base pair changes were confirmed on genomic DNA of 20 phenotypically mutant and 20 sibling larvae for each allele (Figure 3G). For both alleles, the derived hypothetical proteins are truncated and lack the transmembrane domain and the intracellular part containing the tyrosine kinase domain (Figure 3H).

In summary, meiotic mapping of *t20257* revealed close linkage to *flk1*. Sequencing showed premature stop codons in both alleles. The mutant phenotype could be copied by injecting antisense morpholino oligonucleotides. Therefore, we conclude that *t20257* and *t21588* are allelic to *flk1*.

The Expression of *flk1*, but Not of Other Markers for Vasculogenesis and Hematopoiesis, Is Affected in *flk1*^{t20257} Mutant Embryos

To analyze hematopoiesis and vasculogenesis in the progeny of heterozygous *flk1*^{t20257} carriers, we performed in situ hybridizations using markers specific for these processes (*scl*, *gata1*, *fli1*, *vegf*, and *flk1*). Subsequently, individual embryos were genotyped. At the 7-somite stage, all embryos with a mutant genotype (n = 10) displayed a strong reduction of *flk1* expression (Figures 4A and 4B). In contrast, the expression of *scl*, *fli1*, *vegf*, and *gata1* was indistinguishable between sibling and mutant larvae (n = 80 for each probe; Figures 4C–4F, data for *vegf* and *gata1* are not shown).

At 28 hpf, *flk1* expression was still downregulated in all mutant embryos (n = 16) compared to sibling larvae (n = 56; Figures 4G and 4H). The expression of *scl*, *gata1*, and *vegf* was unaltered (data not shown). In mutant embryos, *fli1* staining demarcated the main circulatory routes as it did in siblings (Figures 4I and 4J). The only exceptions were the sprouts of the forming Se that were missing in 60% of the mutant embryos (n = 17), and this difference reflects the reduction of these vessels in mutants.

Flk1 Function Is Necessary for the Formation of Additional Vessels upon *vegf*$_{121+165}$ Overexpression

To test whether the Flk1 receptor is required for VEGF signal transduction, we injected *vegf*$_{165}$ DNA constructs into embryos derived from heterozygous *flk1*^{t20257} carriers. This resulted in high expression levels of *vegf*$_{165}$ mRNA in the yolk, while ectopic expression in other

regions of the embryo was not detectable, as examined by in situ hybridization (data not shown). A total of 432 embryos from 10 different heterozygous matings were injected with 50 pg DNA, and the vasculature was visualized. Almost all vessels were unchanged. Only the SIV showed the formation of additional vessels between the SIV and the common cardinal vein (Figures 5A and 5C). This effect could be observed in 16.5% ± 10.5% of the larvae, while 24.0% ± 6.0% showed a mutant SIV (Figure 5B). Genotyping revealed that all specimens with additional vessels were heterozygous or wild-type (n = 52). In contrast, mutant larvae never formed additional vessels, but the SIV remained thin and the number of branches was still reduced (n = 79).

Similar results were observed when overexpressing a 1:1 mixture of $vegf_{165}$ and $vegf_{121}$. A total of 241 embryos from 7 different heterozygous matings were injected with an approximate total of 50 pg DNA. Additional sprouts were observed in 32.4% ± 15.5% of the larvae (Figure 5D), while 22.8% ± 8.4% displayed a mutant SIV. Genotyping showed that all larvae with surplus vessels were heterozygous or wild-type (n = 72).

Overexpression of $vegf_{165}$ or a mixture of $vegf_{121}$ and $vegf_{165}$ is sufficient to cause the outgrowth of additional vessels in wild-type embryos. However, *flk1* mutant larvae did not respond to such a VEGF stimulus with the formation of additional sprouts, and the SIV was not restored.

Discussion

The alkaline phosphatase activity-based staining assay allowed a more sensitive detection of vascular defects than in the first large-scale zebrafish screens [18, 19]. By this means, we performed, to our knowledge, the largest forward genetic screen for genes involved in vertebrate blood vessel formation.

Phenotypic analysis of $flk1^{t20257}$ has shown that the formation of the initial circulatory loops in the trunk and tail occurs normally. After this time point, the first alterations become visible on a molecular level. The sprouts of the Se cannot be detected in *fli1* in situ hybridizations of *flk1* mutant embryos. This defect is mirrored on a morphological level, since, in *flk1* mutants, the Se fail to form in approximately half of the somite boundaries. Other vessels that are either affected in their formation or function are the central arteries, the blood supply of the digestive system (most prominently the SIV), and the pectoral artery and vein. These vessels are probably generated by sprouting angiogenesis [10, 12]. A failure in sprouting might also explain the observed accumulations of erythrocytes around the swim bladder in $flk1^{t20257}$ mutants, since the formation of the blood vessel plexus on the swim bladder occurs around 3 dpf. The blood pools around the eye might involve the formation of lacunae in the choroid plexus comparable with the changes of the lateral dorsal aorta. These alterations might be explained by impaired remodeling of blood vessels and are the subject of further studies.

In zebrafish, only one VEGF receptor has been identified so far. Based on alignments and BLAST analysis of partial sequence information, it has been named *flk1*, suggesting that this gene is the zebrafish ortholog of the mammalian Flk1 [14–17]. However, analyzing the full-length sequence of the zebrafish VEGF receptor by using ClustalW and BLAST reveals a closer relationship to mammalian Flt1 than to mammalian Flk1 (data not shown). When comparing the extracellular domain and the kinase domain separately, the results are contradictory, since the extracellular domain shows higher similarity with mammalian Flt1, while the kinase domain is more similar to mammalian Flk1. Therefore, it has been suggested that the published zebrafish VEGF receptor either represents an ancestor of both the Flk1 and Flt1 genes or a third receptor distinct from Flk1 and Flt1 [14–17]. At the moment, this question cannot be resolved. We feel that it is likely that the nomenclature will have to be changed once the complete genomic sequence is available.

The extracellular parts of the mammalian VEGF receptors Flk1 and Flt1 comprise seven Ig-like domains. Analysis of the zebrafish VEGF receptor by using PFam identifies only six instead of seven Ig-like domains, possibly reflecting the absence of the second Ig-like domain in zebrafish. However, a comparison of the extracellular part of zebrafish *flk1* with human KDR shows a very high similarity between the second human Ig-like domain and the corresponding zebrafish sequence. We therefore suggest that the zebrafish VEGF receptor comprises seven Ig-like domains.

The ligand binding function of the Flt1 and Flk1 receptors resides within the first four Ig-like domains [20–24]. In both identified mutant *flk1* alleles, premature stop codons presumably lead to a truncated protein comprising the first four or five Ig-like domains, respectively. Therefore, a truncated Flk1 receptor might retain some VEGF binding activity in mutant embryos. However, the morpholino knockdown of *flk1* phenocopies the chemically induced mutations. In addition, *flk1* transcripts are almost absent in *flk1* mutant embryos, probably due to nonsense-mediated mRNA decay. These findings strongly suggest that $flk1^{t20257}$ and $flk1^{t21588}$ represent null mutations.

The loss of *flk1* in zebrafish does not disturb vasculogenesis and hematopoiesis but specifically disrupts angiogenic sprouting of blood vessels from preexisting vessels. This phenotype differs from the results of gene targeting experiments for both Flk1 and Flt1 in mouse [6–8]. These discrepancies might be explained by the differences during embryonic blood vessel formation between zebrafish and mouse. While in mouse embryos a primary vessel plexus is formed and subsequently remodeled, the main vessels in zebrafish form directly without apparent remodeling [12].

Overexpression of $vegf_{121}$ and $vegf_{165}$ mRNA stimulates the differentiation of endothelial cells and hematopoiesis [25]. Here, we demonstrate that ectopic overexpression of $vegf_{165}$ or $vegf_{121+165}$ induces the formation of additional vessels in wild-type zebrafish larvae, mimicking a similar response to VEGF in other vertebrates [26–28]. However, in the absence of a wild-type Flk1 receptor, additional blood vessels are never observed, confirming that zebrafish *flk1* is necessary for VEGF-induced sprouting of new blood vessels. Comparing the injection of $vegf_{165}$ and the coinjection of $vegf_{121+165}$

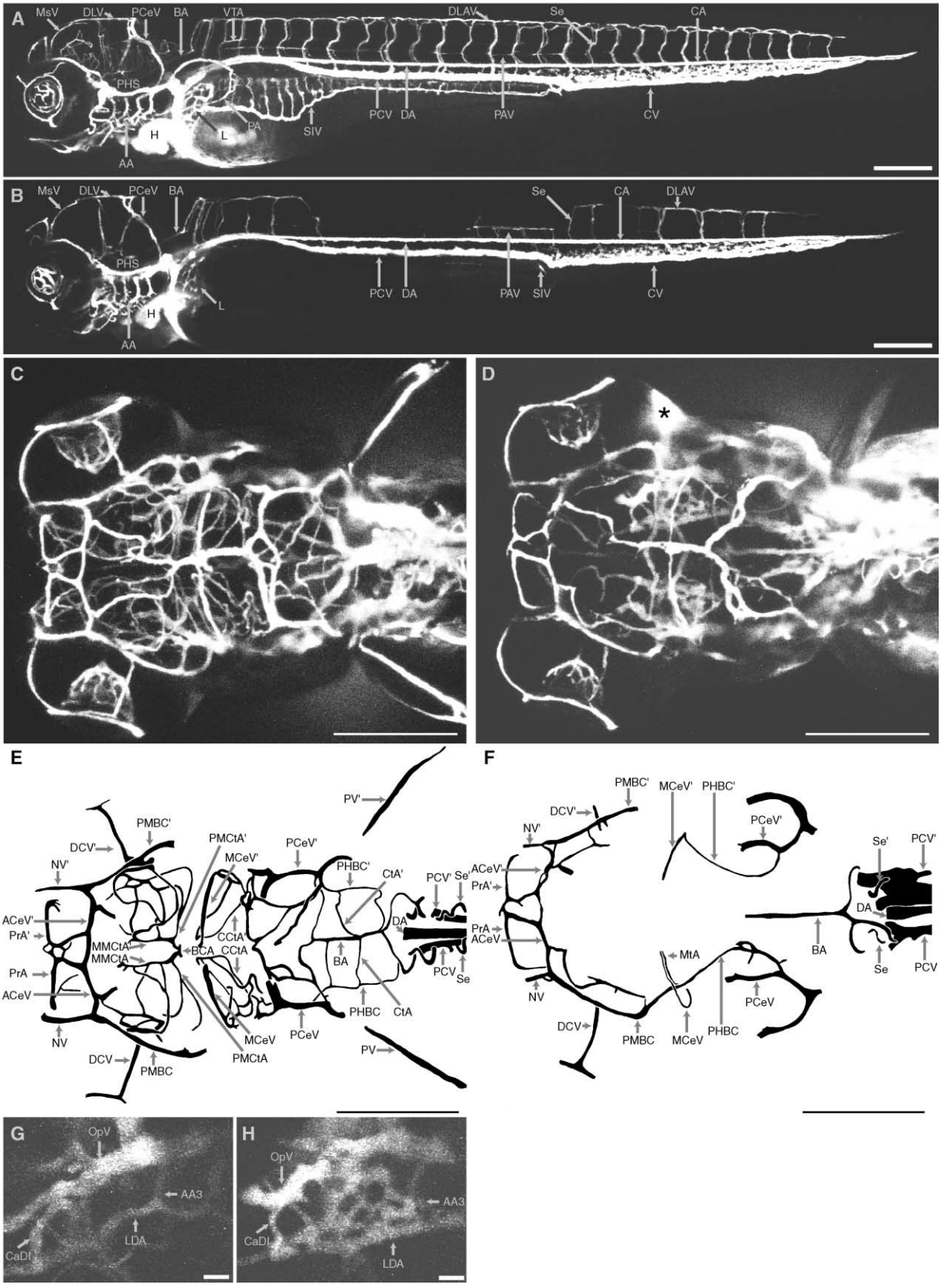
A
MsV
DLV
PCeV
BA
VTA
DLAV
Se
CA
PHS
H
L
PA
SIV
PCV
DA
PAV
CV
AA
B
MsV
DLV
PCeV
BA
Se
CA
DLAV
PHS
H
L
PCV
DA
PAV
SIV
CV
AA
C
D
*
E
PV'
PMBC'
DCV'
NV'
PMCtA'
MCeV'
PCeV'
PHBC'
CtA'
PCV'
Se'
ACeV'
PrA'
DA
MMCtA'
MMCtA
BCA
CCtA'
CCtA
BA
PCV
Se
PrA
ACeV
PHBC
CtA
NV
MCeV
PCeV
DCV
PMBC
PMCtA
PV
F
PMBC'
MCeV'
PHBC'
DCV'
NV'
PCeV'
Se'
PCV'
ACeV'
PrA'
DA
PrA
ACeV
MtA
BA
Se
PCV
NV
PCeV
DCV
PMBC
MCeV
PHBC
G
OpV
AA3
LDA
CaDI
H
OpV
AA3
CaDI
LDA

shows that overexpressing both isoforms is more potent in inducing the formation of surplus blood vessels, and this also confirms published results.

In approximately 20% of the *vegf*-injected embryos, we observed a dilation of the main vessels in the trunk and tail combined with a pooling of erythrocytes in the caudal vein (data not shown). However, we could not determine whether this accumulation of erythrocytes reflected a stimulation of hematopoiesis or erythropoieses or was caused by the described dilation of the vessel lumen.

Loss of VEGF function in zebrafish induced by VEGF morpholino injection affects the entire vasculature, including the dorsal aorta and the posterior cardinal vein [29], and thus has a much stronger effect on vasculogenesis compared to the loss of function of its receptor. A possible explanation for this might be the existence of a second VEGF receptor. This hypothesis is supported by the fact that, in mouse, loss of VEGF function has a much stronger effect on vessel formation than the loss of either VEGF receptor [2].

Conclusions

Molecular cloning of a *flk1* mutation reveals the specific role of this receptor in blood vessel development in zebrafish. While vasculogenesis and hematopoiesis are apparently not affected in *flk1* mutants, the loss of *flk1* function impairs the formation of blood vessels generated by sprouting. Overexpression of $vegf_{121+165}$ demonstrates that Flk1 is necessary for the sprouting of additional vessels in response to VEGF. Therefore, *flk1* is required for angiogenesis in zebrafish.

Supplementary Material

Supplementary Material including the Experimental Procedures is available at http://images.cellpress.com/supmat/supmatin.htm.

Acknowledgments

We thank J.-N. Chen for comments on the alkaline phosphatase-staining protocol; H. Hufnagel for help during the screen; P. Beeckmann, C. Prieβnitz, and T. Wagner for supporting the mapping of *t20257*; I. Görcke and L. Schleithoff for performing 5'RACE; H. Tintrup for assistance with sequencing; E. Weinberg for the $vegf_{165}$ construct; A.M. Küchler for the $vegf_{121}$ construct; AVI BioPharma for providing morpholinos; and G. Stott and A.M. Vogel for discussions and comments on the manuscript.

Received: March 1, 2002
Revised: May 28, 2002
Accepted: July 1, 2002
Published: August 20, 2002

References

1. Risau, W., and Flamme, I. (1995). Vasculogenesis. Annu. Rev. Cell Dev. Biol. *11*, 73–91.
2. Risau, W. (1997). Mechanisms of angiogenesis. Nature *386*, 671–674.
3. Carmeliet, P. (2000). Mechanisms of angiogenesis and arteriogenesis. Nat. Med. *6*, 389–395.
4. Carmeliet, P., Ferreira, V., Breier, G., Pollefeyt, S., Kieckens, L., Gertsenstein, M., Fahrig, M., Vandenhoeck, A., Harpal, K., Eberhardt, C., et al. (1996). Abnormal blood vessel development and lethality in embryos lacking a single VEGF allele. Nature *380*, 435–439.
5. Ferrara, N., Carver-Moore, K., Chen, H., Dowd, M., Lu, L., O'Shea, K.S., Powell-Braxton, L., Hilla, K.J., and Moore, M.W. (1996). Heterozygous embryonic lethality induced by targeted inactivation of the VEGF gene. Nature *380*, 439–442.
6. Shalaby, F., Rossant, J., Yamaguchi, T.P., Gertsenstein, M., Wu, X.F., Breitman, M.L., and Schuh, A.C. (1995). Failure of blood-island formation and vasculogenesis in Flk-1-deficient mice. Nature *376*, 62–66.
7. Fong, G.H., Rossant, J., Gertsenstein, M., and Breitman, M.L. (1995). Role of the Flt-1 receptor tyrosine kinase in regulating the assembly of vascular endothelium. Nature *376*, 66–70.
8. Fong, G.H., Zhang, L., Bryce, D.M., and Peng, J. (1999). Increased hemangioblast commitment, not vascular disorganization, is the primary defect in flt-1 knock-out mice. Development *126*, 3015–3025.
9. Romeis, B. (1989). *Mikroskopische Technik,* 17th Edition (München: Urban u. Schwarzenberg).
10. Childs, S., Chen, J.N., Garrity, D.M., and Fishman, M.C. (2002). Patterning of angiogenesis in the zebrafish embryo. Development *129*, 973–982.
11. Weinstein, B.M., Stemple, D.L., Driever, W., and Fishman, M.C. (1995). Gridlock, a localized heritable vascular patterning defect in the zebrafish. Nat. Med. *1*, 1143–1147.
12. Isogai, S., Horiguchi, M., and Weinstein, B.M. (2001). The vascular anatomy of the developing zebrafish: an atlas of embryonic and early larval development. Dev. Biol. *230*, 278–301.
13. Geisler, R., Rauch, G.J., Baier, H., van Bebber, F., Brobeta, L., Dekens, M.P., Finger, K., Fricke, C., Gates, M.A., Geiger, H., et al. (1999). A radiation hybrid map of the zebrafish genome. Nat. Genet. *23*, 86–89.
14. Fouquet, B., Weinstein, B.M., Serluca, F.C., and Fishman, M.C. (1997). Vessel patterning in the embryo of the zebrafish: guidance by notochord. Dev. Biol. *183*, 37–48.
15. Liao, W., Bisgrove, B.W., Sawyer, H., Hug, B., Bell, B., Peters, K., Grunwald, D.J., and Stainier, D.Y. (1997). The zebrafish gene cloche acts upstream of a flk-1 homologue to regulate endothelial cell differentiation. Development *124*, 381–389.

Figure 2. All Vessels that Are Affected in *t20257* Mutant Larvae Form Later than 36 hr Postfertilization in the Wild-Type

(A–H) Confocal microangiography of a (A, C, E, and G) sibling larva and a (B, D, F, and H) *t20257* mutant larva at 4 dpf. (A and B) A lateral view, (C and D) a dorsal view of the head, (E and F) a schematic drawing of a subset of the head vessels, (G and H) and a blow-up of the right lateral dorsal aorta. (A and B) In the trunk and tail, the dorsal aorta (DA), caudal artery (CA), caudal vein (CV), and posterior cardinal vein (PCV) are indistinguishable between siblings and mutants. The mutant heart (H) is slightly smaller. Despite the lack of a functional subintestinal vein (SIV), a network of small channels forms in the developing liver (L). (C–F) In the head, the vessels forming before 1.5 dpf, e.g., the prosencephalic artery (PrA), the anterior cerebral vein (ACeV), or the basilar artery (BA), are normally developed. However, in mutant larvae, the central arteries (CtA) are not detectable. (G and H) The vessels shown are located underneath the vessels labeled MCeV′ in Figures 2E and 2F. In mutant larvae, the lateral dorsal aorta (LDA) forms a vascular plexus. Other abbreviations used include: asterisk, accumulation of fluorescent dye; AA, aortic arches; AA3, first branchial arch; BCA, basal communicating artery; CaDI, caudal division of the internal carotid artery; CCtA, cerebellar central artery; DCV, dorsal ciliary vein; DLAV, dorsal longitudinal anastomotic vessel; DLV, dorsal longitudinal vessels; MCeV, middle cerebral vein; MMCtA, middle mesencephalic central artery; MsV, mesencephalic vein; MtA, metencephalic artery; NV, nasal vein; OpV, ophthalmic vein; PAV, parachordal vessel; PCeV, posterior cerebral vein; PHBC, primordial hindbrain channel; PHS, primary head sinus; PMBC, primordial midbrain channel; PMCtA, posterior mesencephalic central artery; Se, intersegmental vessel; and VTA, vertebral artery. The scale bar represents 200 μm in (A)–(F) and 20 μm in (G) and (H).

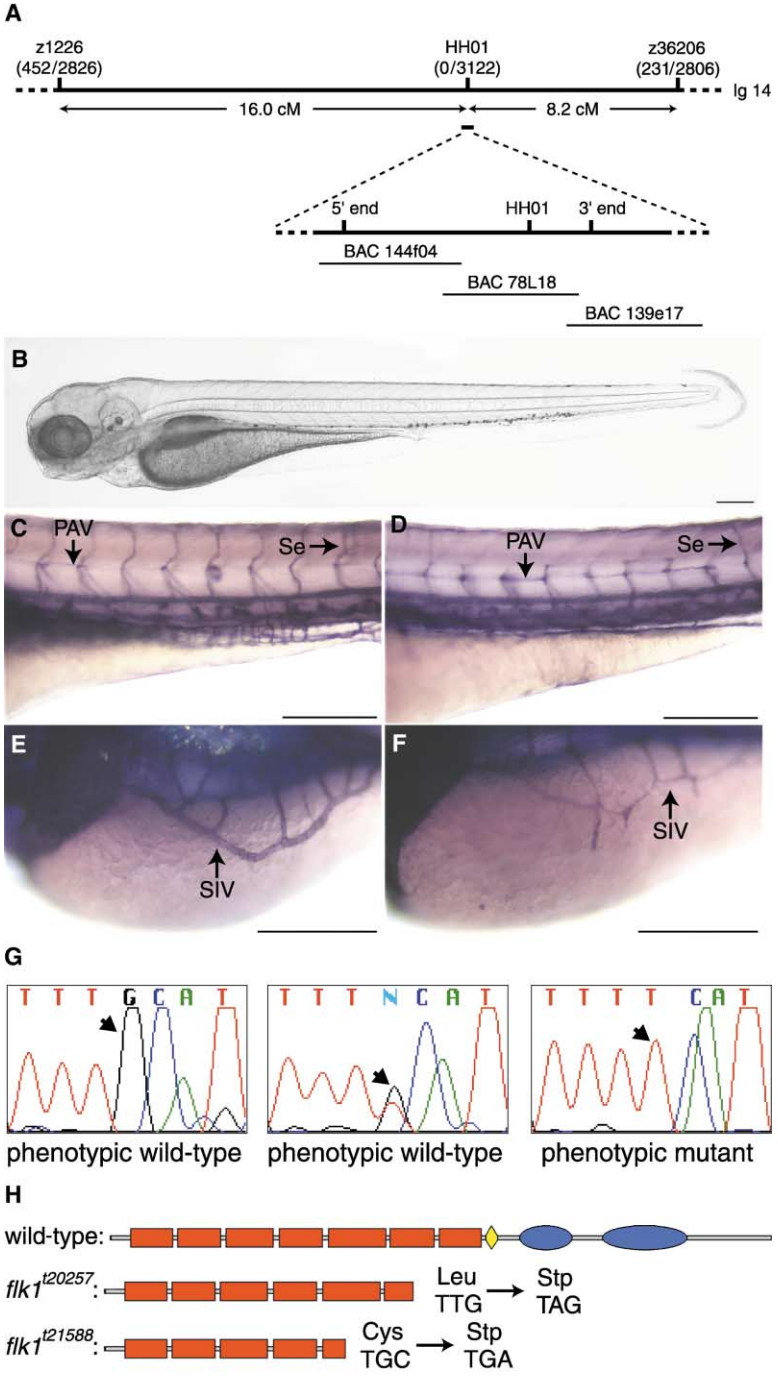

Figure 3. *t20257* and *t21588* Are Mutant Alleles of the Gene Published as *flk1*

(A) Meiotic mapping with microsatellite markers placed *t20257* on linkage group 14 between the markers z1226 and z36206. A contiguous stretch of genomic DNA was assembled covering the entire *flk1* locus. For the marker HH01, no recombinants were found. The numbers of recombinants per analyzed meioses are shown in brackets.

(B–F) Knockdown of *flk1* by injecting an antisense morpholino oligonucleotide targeting the 5′ UTR of the *flk1* mRNA results in a phenocopy of the *t20257* and *t21588* mutations. (B, D, and F) Larvae injected with 4.5 ng antisense morpholino oligonucleotide; (C and E) control larvae. (B) The overall morphology is not affected at 4 dpf, (C–F) but alkaline phosphatase staining reveals the same changes of the intersegmental vessels (Se), the parachordal vessels (PAV), and the subintestinal vein (SIV) that can be observed in the ENU-induced mutations. The scale bars represent 200 μm.

(G) Sequencing the genomic DNA of single larvae confirms the point mutation detected in the cDNA of *t21588* mutant larvae: larvae with a wild-type vasculature are either homozygous for a G at the site of interest or are heterozygous G/T. Larvae with a mutant vasculature are always homozygous for T at the site of interest.

(H) The point mutations in *t20257* and *t21588* both result in nonsense codons. Red boxes, Ig-like domains; yellow diamond, transmembrane domain; blue ovals, tyrosine kinase domains.

16. Sumoy, L., Keasey, J.B., Dittman, T.D., and Kimelman, D. (1997). A role for notochord in axial vascular development revealed by analysis of phenotype and the expression of VEGR-2 in zebrafish flh and ntl mutant embryos. Mech. Dev. *63*, 15–27.
17. Thompson, M.A., Ransom, D.G., Pratt, S.J., MacLennan, H., Kieran, M.W., Detrich, H.W., III, Vail, B., Huber, T.L., Paw, B., Brownlie, A.J., et al. (1998). The cloche and spadetail genes differentially affect hematopoiesis and vasculogenesis. Dev. Biol. *197*, 248–269.
18. Stainier, D.Y., Fouquet, B., Chen, J.N., Warren, K.S., Weinstein, B.M., Meiler, S.E., Mohideen, M.A., Neuhauss, S.C., Solnica-Krezel, L., Schier, A.F., et al. (1996). Mutations affecting the formation and function of the cardiovascular system in the zebrafish embryo. Development *123*, 285–292.
19. Chen, J.N., Haffter, P., Odenthal, J., Vogelsang, E., Brand, M., van Eeden, F.J., Furutani-Seiki, M., Granato, M., Hammerschmidt, M., Heisenberg, C.P., et al. (1996). Mutations affecting the cardiovascular system and other internal organs in zebrafish. Development *123*, 293–302.
20. Davis-Smyth, T., Chen, H., Park, J., Presta, L.G., and Ferrara, N. (1996). The second immunoglobulin-like domain of the VEGF tyrosine kinase receptor Flt-1 determines ligand binding and

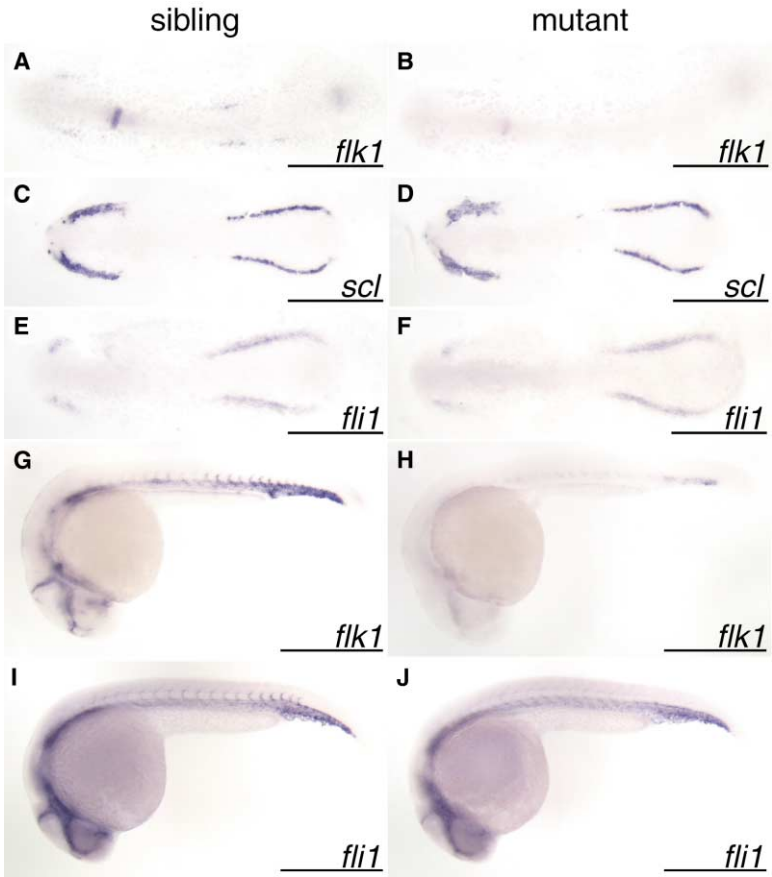

Figure 4. *flk1* Is Not Required for the Early Expression of *scl* and *fli1*

(A–J) Whole-mount in situ hybridizations of (A, C, E, G, and I) sibling and (B, D, F, H, and J) mutant larvae using (A, B, G, and H) *flk1*, (C and D) *scl*, and (E, F, I, and J) *fli1* as probes to detect the respective mRNAs. (A–F) A dorsal view of flat-mounted embryos at the 7-somite stage; (G–J) a lateral view of 28-hpf embryos. (A, B, G, and H) Mutant larvae showed a strongly reduced expression of *flk1* both at the 7-somite stage and at 28 hpf. (C–F) The expression of *scl* and *fli1* is indistinguishable between embryos with either a mutant or a sibling genotype at the 7-somite stage. At 28 hpf, *fli1* expression in mutant embryos resembles the wild-type expression pattern, with the exception of the forming intersegmental vessels, which are not stained. Anterior is oriented toward the left; the scale bars represent 500 μm.

may initiate a signal transduction cascade. EMBO J. *15*, 4919–4927.

21. Barleon, B., Totzke, F., Herzog, C., Blanke, S., Kremmer, E., Siemeister, G., Marme, D., and Martiny-Baron, G. (1997). Mapping of the sites for ligand binding and receptor dimerization at the extracellular domain of the vascular endothelial growth factor receptor FLT-1. J. Biol. Chem. *272*, 10382–10388.
22. Cunningham, S.A., Stephan, C.C., Arrate, M.P., Ayer, K.G., and Brock, T.A. (1997). Identification of the extracellular domains of Flt-1 that mediate ligand interactions. Biochem. Biophys. Res. Commun. *231*, 596–599.
23. Wiesmann, C., Fuh, G., Christinger, H.W., Eigenbrot, C., Wells, J.A., and de Vos, A.M. (1997). Crystal structure at 1.7 Å resolution of VEGF in complex with domain 2 of the Flt-1 receptor. Cell *91*, 695–704.
24. Shinkai, A., Ito, M., Anazawa, H., Yamaguchi, S., Shitara, K., and Shibuya, M. (1998). Mapping of the sites involved in ligand association and dissociation at the extracellular domain of the kinase insert domain-containing receptor for vascular endothelial growth factor. J. Biol. Chem. *273*, 31283–31288.
25. Liang, D., Chang, J.R., Chin, A.J., Smith, A., Kelly, C., Weinberg, E.S., and Ge, R. (2001). The role of vascular endothelial growth factor (VEGF) in vasculogenesis, angiogenesis, and hematopoiesis in zebrafish development. Mech. Dev. *108*, 29–43.

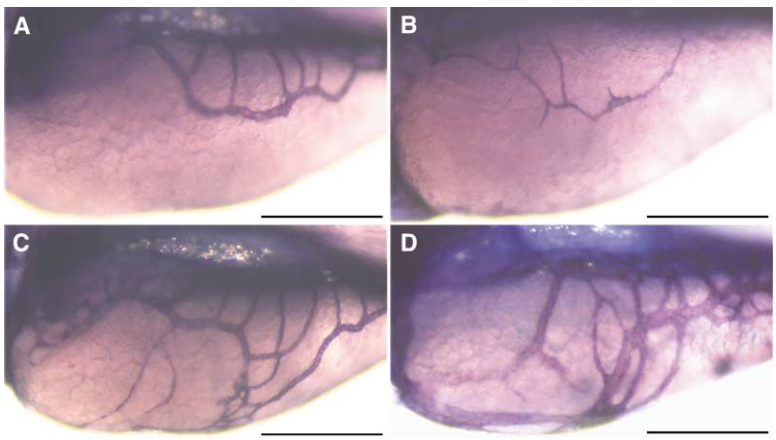

Figure 5. Overexpression of $vegf_{165}$ or $vegf_{121+165}$ Promotes the Outgrowth of Additional SIV Branches in Wild-Type, but Not in *flk1* Mutant Larvae

(A–D) Alkaline phosphatase staining of the subintestinal vein (SIV) of 4-dpf-old progeny of heterozygous $flk1^{t20257}$ carriers injected with a (A) control DNA, with a (B and C) $vegf_{165}$-construct, or a (D) 1:1 mixture of DNA encoding $vegf_{121}$ and $vegf_{165}$. (A) While, in controls, the formation of additional sprouts was never observed, (C and D) the injection of the $vegf_{165}$ construct and the coinjection of $vegf_{121}$ and $vegf_{165}$ led to the outgrowth of surplus vessels. (B) Approximately 25% of the larvae display the mutant phenotype. The scale bars represent 200 μm.

26. Flamme, I., von Reutern, M., Drexler, H.C., Syed-Ali, S., and Risau, W. (1995). Overexpression of vascular endothelial growth factor in the avian embryo induces hypervascularization and increased vascular permeability without alterations of embryonic pattern formation. Dev. Biol. *171*, 399–414.
27. Wilting, J., Birkenhager, R., Eichmann, A., Kurz, H., Martiny-Baron, G., Marme, D., McCarthy, J.E., Christ, B., and Weich, H.A. (1996). VEGF121 induces proliferation of vascular endothelial cells and expression of flk-1 without affecting lymphatic vessels of chorioallantoic membrane. Dev. Biol. *176*, 76–85.
28. Cleaver, O., Tonissen, K.F., Saha, M.S., and Krieg, P.A. (1997). Neovascularization of the *Xenopus* embryo. Dev. Dyn. *210*, 66–77.
29. Nasevicius, A., Larson, J., and Ekker, S.C. (2000). Distinct requirements for zebrafish angiogenesis revealed by a VEGF-A morphant. Yeast *17*, 294–301.

Accession Numbers

The full-length sequence of *flk1* is published under GenBank accession number AF487829.